Dual-axis manual control

Performance degradation, axis asymmetry, crossfeed, and intermittency

Barendswaard, Sarah; Pool, Daan Marinus; Van Paassen, Marinus M.; Mulder, Max

DOI
10.1109/THMS.2019.2890856

Publication date
2019

Document Version
Accepted author manuscript

Published in
IEEE Transactions on Human-Machine Systems

Citation (APA)
Barendswaard, S., Pool, D. M., Van Paassen, M. M., & Mulder, M. (2019). Dual-axis manual control: Performance degradation, axis asymmetry, crossfeed, and intermittency. *IEEE Transactions on Human-Machine Systems*, *49*(2), 113-125. Article 8624395. https://doi.org/10.1109/THMS.2019.2890856

Dual-Axis Manual Control: Performance Degradation, Axis Asymmetry, Crossfeed, and Intermittency

Sarah Barendswaard, Daan Marinus Pool, *Member, IEEE*, Marinus M. Van Paassen, *Senior Member, IEEE*, and Max Mulder, *Member, IEEE*

***Abstract*—Vehicle control tasks require simultaneous control of multiple degrees-of-freedom. Most multi-axis human-control modeling is limited to the modeling of multiple fully independent single axes. This paper contributes to the understanding of multi-axis control behavior and draws a more realistic and complete picture of dual-axis manual control. A human-in-the-loop experiment was performed to study four distinctive phenomena that can occur in multi-axis control: performance degradation, axis asymmetry, crossfeed, and intermittency. In a simulator, three conditions were tested in the presence and absence of physical motion: the full dual-axis control task, single-axis roll task, and single-axis pitch task. Controlled element dynamics, stick dynamics, and forcing functions were equal in all cases. Results show that performance is worse in dual-axis tasks. Performance in roll axis is consistently worse than pitch, thereby proving axis asymmetry. Physical motion improves the performance and stability of the system. The application of independent forcing function signals in both controlled axes resulted in the detection of crossfeed in dual-axis tasks from spectral analysis. Using a novel extended Fourier coefficient method, the identified crossfeed dynamics can explain up to 20% of the measured control inputs and improves modeling accuracy by up to 5%. Dual-axis control behavior is less accurately modeled with linear time-invariant models and is more intermittent.**

***Index Terms*—Crossfeed, cybernetics, dual axis, manual control, man-machine systems, modeling.**

I. Introduction

DESPITE the fact that most operationally relevant manual control tasks–especially those in the vehicle domain–typically require human controllers (HC) to perform simultaneous control of multiple degrees-of-freedom, our understanding of the intricacies of such multi-axis control is still severely limited. In fact, the current state-of-the-art for the analysis and modeling of multi-axis manual control takes accounts only for multiple *independent* single-axis tasks [1]–[4]. While somewhat successful, such approaches cannot account for the inherently multi-input-multi-output nature of the HC in a multi-axis case. Furthermore, due to task and operator limitations, additional multi-axis phenomena may occur. We argue that for meaningful understanding and prediction of human operator performance in multi-axis tasks, the presence of such phenomena needs to be verified, if not explicitly accounted for in our analysis methods and operator models.

Early investigations into human control in dual-axis tasks have shown that marked differences with single-axis manual control do indeed exist [1], [5]–[8]. Degraded task performance has been reported in dual-axis tracking, in addition to increased operator remnant and nonlinear control behavior levels [6]. Furthermore, a focus on one axis or a consistent prioritization has been observed [9], an effect referred to as axis asymmetry. While some studies have postulated that such asymmetry may be explained by a systematic reduction in operator aggressiveness (reduced crossover frequency) compared to the single-axis case [10], [11], others have proposed that the characterization of multi-axis control should include task interference phenomena, such as those resulting from divided attention (e.g., switching between axes), prioritization between axes–axis asymmetry [9] and time varying axis prioritization–intermittency [1]. A number of earlier investigations [1], [5], [7], have proposed to analyze and model *crossfeed* between axes, which occurs when operators are unable to fully decouple their separate tasks. The first study to date that has successfully used objective human operator identification techniques to verify the presence and dynamics of the hypothesized crossfeed is in the preliminary paper [12]. This study needs significant elaboration in crossfeed, through quantifying the crossfeed response by parametric identification, and by investigating the other postulated in dual axis: nonlinear intermittency, performance degradation and axis asymmetry.

The state-of-the-art has not been able to open up the black box of human control in dual-axis tracking and only focused on performance, control activity, and time domain metrics [1], [9]. These do not dissect the HC response in the multiple axes, instead lumping all responses. This means that in the design of interfaces that intend to support HC's in manual control multiaxes tasks (such as in aircraft or helicopter control, where one manipulator is typically used to control two or even three "dimensions" of vehicle movement) we have no idea how strong the effects of crossfeed, axis asymmetry, performance degradation, and intermittency are, so we also cannot compensate for these phenomena in a systematic fashion. For the case of

Manuscript received July 31, 2017; revised May 15, 2018; accepted November 17, 2018. This paper was recommended by Associate Editor S. Landry. *(Corresponding author: Sarah Barendswaard.)*

The authors are with the Department Control and Operations, Delft University of Technology, Delft 2628, The Netherlands (e-mail: s.barendswaard@tudelft.nl; d.m.pool@tudelft.nl; m.m.vanpaassen@tudelft.nl; m.mulder@tudelft.nl).

Digital Object Identifier 10.1109/THMS.2019.2890856

helicopters, this may be an even larger issue, crossfeed could result in possibly even bigger undesired effects in the closed loop with the already existing asymmetrical cross-coupled dynamics [13].

This investigation narrows its focus from multi-axis to only dual-axis manual control. Following the traditional (quasi-linear) analysis of human control behavior [3], this paper studies the fundamental characteristics of human behavior in dual-axis manual control, through a representative yet abstracted experiment where human behavior is sufficiently linear and time-invariant to allow for its objective analysis with linear time invariant (LTI) human control identification and modeling techniques [14].

To achieve this, this paper introduces and extends modern identification techniques to analyze the occurrence and nature of crossfeed and intermittency in manual dual-axis control, using a model-based approach. A human-in-the-loop experiment is performed in the SIMONA Research Simulator (SRS), TU Delft, to collect measurements of human operators in a simulated aircraft dual-axis roll and pitch control task with physical motion feedback. Application of two independent multisine forcing functions in each controlled axis facilitates the *detection* of crossfeed through analysis of measured signals with spectral methods [15]. Furthermore, the multichannel human operator identification method developed by [16] is newly extended, as in [12], to objectively *identify* the dynamics of the additional crossfeed responses (nonparametrically) and the changes in other responses. Based on this nonparametric identification, parametric modeling of the crossfeed response is performed for the first time. In addition, to detect possible intermittency in dual-axis control, we explicitly compare the occurrence of instantaneous large fitting errors for our LTI human control models–indicative of expected but "missing" control inputs in the experiment data–between single and dual-axis conditions. Performance degradation and axis asymmetry are investigated by comparing the performance metrics; error variance, control variance, crossover frequency, and phase margin, along with the parameter estimates, for both axis type and axis dimension.

This paper is structured as follows. Background information can be found in Section II. The dual-axis control task, experimental design, and the system identification approach are elaborated in Sections III and IV, respectively. Results are presented in Section V and the paper ends with a discussion and conclusions in Section VI and VII, respectively.

II. Background

Single and dual-axis tasks are critically different. There are four main additional phenomena that come into play with dual-axis (compared to single-axis control) in literature: i) performance degradation, ii) crossfeed, iii) asymmetry, and iv) intermittency. Understanding and, if possible modeling these four phenomena forms the focus of this paper.

Multiple investigations have clearly found a *degradation in performance* with dual axis in comparison to single axis tasks [1], [7], [17]. In fact, the relation between crossover frequency (the frequency up to which the HC is able to track) and the number of axis was postulated to be proportional to the reciprocal of the square root of the number of axis [18]. That is, with dual axes, the crossover frequency is $1/\sqrt{2}$ of that of the single axes case. A similar relation deduced by [11] states that the crossover frequency is proportional to the reciprocal of the number of axes used. These relations are based on modeling the human brain as a multichannel processor, the more channels being used, the less amount of continuous attention given to each of the tasks [19], [20].

Asymmetry of manual control behavior in each axis is shown by the performance measures being distinctly different in each axis, even with equal controlled element dynamics [1]. This can be a consequence of the differences in visual representation, control manipulator design, or emphasis on a particular axis during training, or different overall lumped neuromuscular properties in each axis [21]. Furthermore, it can also result from the human operator consciously prioritizing one axis over the other [9].

Crossfeed is described as a type of task interference, or the human operators' inability to decouple the two tasks. Crossfeed can have motoric causes (e.g., hand geometry, manipulator geometry) affecting the HC's actuation or output dynamics, or perceptual causes (e.g., visual and vestibular thresholds, display resolution, display position) both affecting the HC's inputs. Evidence for *linear time-invariant* perceptual crossfeed was found in a task that used a separate manipulator for each axis [7]. Bekey *et al.* [1] did not find any consistent evidence for crossfeed, rather crossfeed was only found for a short period of time, making the phenomenon time varying. Previous investigations have either used subjective time-domain iterative model matching techniques [1], [5] or open-loop frequency-domain methods [7]. Neither of the techniques used in [1], [5], or [7] could accurately capture the dynamics of crossfeed in the frequency domain, however.

The phenomenon of time-varying prioritization or *intermittency* is found with integrated displays and separated displays alike [17]. When one axis has a larger error than the other, this axis can be (temporarily) prioritized over the other [1], [9]. Intermittent behavior has been found to be smaller with the use of motion [10], thereby producing more consistent, linear time-invariant pilot behavior. Intermittency is traditionally lumped up with pilot remnant [2], and has been found to proportionally increase with each additional axis used [6].

In this paper, we aim to obtain an accurate description of performance degradation and axis asymmetry. Novel metrics are used to detect intermittency: peak time. For crossfeed, an objective extended identification algorithm [16] is used to identify crossfeed nonparametrically first, supplemented with parametric identification of crossfeed for the first time. Finally, the effect of motion on these phenomena is analyzed for the first time.

III. Control Task

The control architecture is elaborated in this section using Fig. 1, illustrating the full control task: dual axis with motion, including its dual-axis display, with all other tasks being

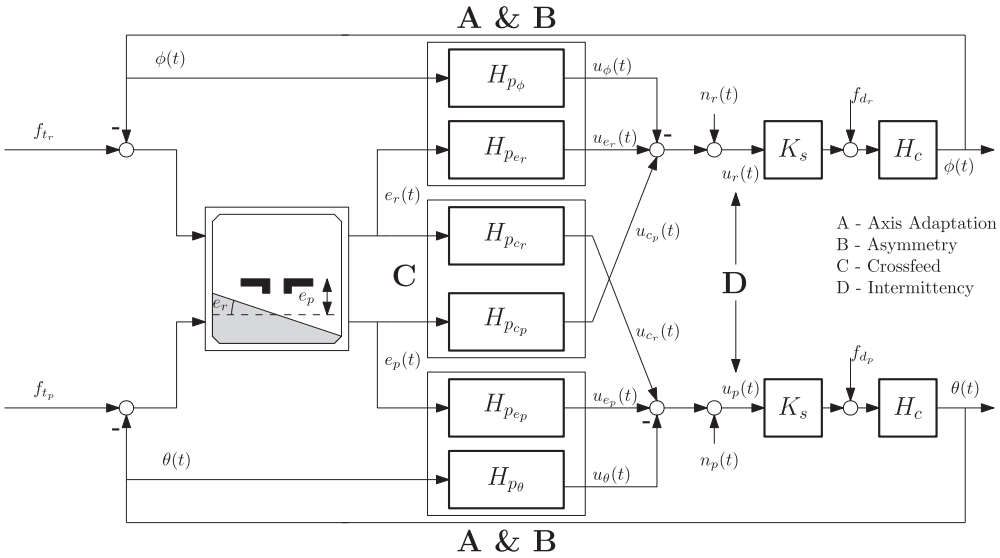

Fig. 1. Schematic representation of a dual-axis tracking task with physical motion feedback and crossfeed.

derivatives. The single axis cases are realized when only considering two independent axis with $H_{p_{e_r}}$ for roll and $H_{p_{e_p}}$ for pitch. With dual axis, the human crossfeed contributions $H_{p_{c_r}}$ and $H_{p_{c_p}}$ are included. Finally, the cases with motion include the additional motion responses H_{p_ϕ} and H_{p_θ}, respectively.

The distinctiveness of this control structure is that it combines the multiple independent single axis with motion from [21] and the crossfeed component from [7].

In our experiment, participants performed both dual-axis and single-axis tasks in the presence and absence of simulator motion. For the dual axis with motion case, the pilot simultaneously controls the aircraft's roll and pitch attitude θ and ϕ as depicted in Fig. 1. For the single-axis cases, the participant would either control roll or pitch. For the sake of identification, our subjects performed a simultaneous target-following and disturbance-rejection task, being excited with two independent forcing functions per axis; f_t and f_d, respectively [22].

The roll and pitch axis tracking errors, e_ϕ and e_θ, were presented on a compensatory visual display matching Fig. 1, similar to an aircraft attitude indicator. It was the participants' task to continuously minimize these tracking errors. Physical roll and pitch motion feedback was taken as vestibular input provided by SIMONA's motion system without any scaling or filtering. Due to the motion limitations of the SRS, the specific forces resulting from simulator rotations, could not be compensated for. However, this effect was very small.

The human can be modeled through six different operator responses: $H_{p_{e_r}}$ and $H_{p_{e_p}}$ respond to the error signals in each respective axis, H_{p_ϕ} and H_{p_θ} respond to the matching vestibular inputs, and the crossfeed responses $H_{p_{c_r}}$ and $H_{p_{c_p}}$ react to the off-axes error signals. Note that this choice for the input to the crossfeed is consistent with earlier work [7], with this convention, it is expected that the dynamics of the crossfeed response will be similar to that of the visual response. The addition of the output of these responses; u_e, u_c, and u_ϕ or u_θ, along with the addition of operator noise $n(t)$, result in the complete operator output: $u_r(t)$ for roll and $u_p(t)$ for pitch. The output is multiplied with the control stick gain K_s, having a fixed value of 0.08, and with the addition of the disturbance, the signals are transformed by the controlled element (CE) H_c.

The specific areas in the control architecture illustrated in Fig. 1 that relate to the four phenomena of interest here, are indicated in the figure as A, B, C, and D. When looking for performance degradation in dual axis, an adaptation of both the performance parameters of the visual and motion blocks in comparison to the baseline single axis case, are focused on, as indicated by A. When looking for axis asymmetry, the HC model parameters and performance of the visual and motion blocks of pitch and roll are compared, as given in B. Crossfeed is found with the existence of a crossfeed transfer block, as given in C. Intermittency can be studied through analyzing the time-domain pilot output signals, as given in D.

The following sections elaborate on particular elements of the control architecture: the controlled element dynamics, forcing functions, and pilot model.

A. *Controlled Aircraft Dynamics*

The aircraft roll and pitch CE dynamics are both defined by H_c as given in Fig. 1. It is found in literature that using cross couplings or different CE dynamics can change the HC control strategy considerably [5], [17]. Therefore, although in real nonlinear aircraft dynamics the roll and pitch axes have different and cross-coupled dynamics, in this investigation, they are kept uncoupled and identical to avoid obscuring the plain differences between single and dual-axis manual control. The dynamics in both axes are defined by a second order transfer function

$$H_c(s) = \frac{67.9}{s(s+3)}. \tag{1}$$

The system defined by (1) is at a transition between single integrator dynamics K/s and double integrator K/s^2 at the frequency 3 rad/s. Therefore, this CE requires the HC to generate mid- to high-frequency lead, which causes them to use physical motion feedback, when available [2], [3]. A break frequency of 3 rad/s was chosen such that the difficulty level of the most demanding tested scenario, i.e., the dual axis no motion task, remains at an acceptable level. Decreasing the break frequency makes the task more challenging, possibly creating a greater distinction between single and dual-axis manual control, but also induces human operator fatigue.

B. Forcing Functions

The target and disturbance forcing functions in both axes were quasi-random multisine signals, as defined by f_{t_r}, f_{t_p}, f_{d_r}, and f_{d_p} in Fig. 1 and by

$$f_{d,t}(t) = \sum_{k=1}^{10} A_{d,t}[k] \sin(\omega_{d,t}[k]t + \phi_{d,t}[k]). \tag{2}$$

Each kth sinusoid in each forcing function is defined by its excitation frequency $\omega_{d,t}[k]$, amplitude $A_{d,t}[k]$, and phase $\phi_{d,t}[k]$. All signals are a sum of 10 sinusoids, spanning frequencies between 0.1 and 20 rad/s, approximately equally spaced on a logarithmic scale. The sampling frequency is 100 Hz and the measurement time equals 81.92 s. The amplitude distribution of the sine components in all forcing functions follows a low-pass filter amplitude distribution:

$$A_{d,k}(k) = \left| \frac{1 + T_{A1} j\omega_{d,t}(k)}{1 + T_{A2} j\omega_{d,t}(k)} \right|^2. \tag{3}$$

Here $T_{A1} = 0.1$ s and $T_{A2} = 0.8$ s identical to those used in [23]. The amplitudes were scaled such that the variance of the target forcing functions is 2.25 deg^2 and that the disturbance signals have a variance of 25% of the target. This ratio of target to disturbance was successfully applied in previous pilot identification investigations [23] and creates a task in which target following is dominant. Disturbance signal amplitudes were prefiltered by the inverse of the CE dynamics as they are inserted into the loop before the CE (see Fig. 1).

Four sets of phases $\phi_{d,t}$ were chosen from a large number of randomly generated phase sets, such that all signals have a Gaussian distribution and an average crest factor, as outlined by the forcing function requirements in [24]. The resulting forcing functions are listed in Tables I and II.

C. Pilot Model

The most elaborate model structure is the dual axis with motion scenario as illustrated in Fig. 1. There are six different operator response functions to consider: two visual response functions, $H_{p_{e_p}}$ and $H_{p_{e_r}}$, the motion responses (in the presence of motion), H_{p_θ} and H_{p_ϕ} and the crossfeed responses (for dual axis), $H_{p_{c_p}}$ and $H_{p_{c_r}}$.

It is known that with a compensatory display the HC adapts their dynamics such that the open-loop dynamics resemble a single-integrator in the crossover region [3]. The visual response in (4) is equivalent to the precision model [2] as appropriate for the CE dynamics given in (1)

$$H_{p_e}(s) = K_v(1 + T_l s)e^{-s\tau_v} \frac{\omega_{\text{nm}}^2}{\omega_{\text{nm}}^2 + 2\zeta_{\text{nm}}\omega_{\text{nm}}s + s^2}. \tag{4}$$

The HC response to motion, models the HC vestibular response

$$H_{p_m} = sK_m e^{-s\tau_m} \frac{\omega_{\text{nm}}^2}{\omega_{\text{nm}}^2 + 2\zeta_{\text{nm}}\omega_{\text{nm}}s + s^2}. \tag{5}$$

Both the motion and visual responses are in line with previous research on dual-axis tracking with motion feedback [23]. The equalization dynamics are defined by the parameters K_v, T_l, and K_m, while the neuromuscular dynamics are defined by a neuromuscular frequency ω_{nm} and damping ζ_{nm}. Delays are defined by a visual τ_v and vestibular τ_m delay. Hence, there are seven parameters per axis. Note that the structure of the HC crossfeed responses H_{p_c} are unknown at this point. These will be determined after discussing the frequency domain identification results in Section V.

TABLE I
PITCH-AXIS FORCING FUNCTION DATA

disturbance, f_{d_p}				target, f_{t_p}			
n_d, –	ω_d, rad/s	A_d, deg	$\phi_{d\phi}$, rad	n_t, –	ω_t, rad/s	A_t, deg	$\phi_{t\phi}$, rad
5	0.384	0.014	1.866	6	0.460	1.657	3.489
11	0.844	0.023	5.013	13	0.997	1.159	0.656
23	1.764	0.027	2.245	27	2.071	0.523	6.169
37	2.838	0.026	3.957	41	3.145	0.282	4.723
51	3.912	0.026	3.538	53	4.065	0.189	0.405
71	5.446	0.028	7.853	73	5.599	0.117	6.201
101	7.747	0.034	5.448	103	7.900	0.074	2.662
137	10.508	0.043	4.108	139	10.661	0.054	0.183
171	13.116	0.055	7.997	194	14.880	0.042	0.607
226	17.334	0.081	6.923	229	17.564	0.039	2.072

TABLE II
ROLL-AXIS FORCING FUNCTION DATA

disturbance, f_{d_r}				target, f_{t_r}			
n_d, –	ω_d, rad/s	A_d, deg	$\phi_{d\phi}$, rad	n_t, –	ω_t, rad/s	A_t, deg	$\phi_{t\phi}$, rad
8	0.614	0.023	3.393	9	0.690	1.681	3.075
15	1.150	0.031	8.851	16	1.227	1.129	5.049
30	2.301	0.032	8.318	31	2.378	0.499	0.760
44	3.375	0.031	8.881	45	3.451	0.283	3.956
55	4.218	0.032	5.259	56	4.295	0.202	3.475
75	5.752	0.034	5.281	76	5.829	0.129	5.546
105	8.053	0.041	5.005	106	8.130	0.084	6.222
141	10.815	0.053	7.486	142	10.891	0.062	0.217
172	13.192	0.066	7.891	195	14.956	0.049	2.639
232	17.794	0.100	3.837	233	17.871	0.045	2.373

IV. METHODOLOGY AND DATA PROCESSING

Data for this investigation are obtained by performing an experiment in the SRS with the control tasks defined in Section III. Here, we describe the experimental methods, data processing techniques, dependent measures, and hypotheses.

A. Experiment Method

1) Independent Variables: Two independent variables were varied in the experiment: axis configuration and motion. Axis configuration has three levels: *single axis pitch*, *single axis roll,* and *dual axis*. Motion has two levels: *motion* and *no motion*. Both crossfeed and intermittency only need the dual-

axis configuration. However, to analyze performance degradation, both the dual-axis and single-axis configurations are needed for comparison. Hence, in total six scenarios are tested.

2) Apparatus and Cueing: The experiment was performed in the SRS. Participants used a Moog FCS Ecol-8000 electrical manipulator stick for giving pitch and roll inputs. The settings of the control loaded manipulator were set to a linear force-displacement characteristic with a stiffness of 1.5 N/deg. The stick was left unlocked for the single-axis cases, to detect possible motoric crossfeed. Control inputs were limited to $\pm 15^{\circ}$, whereas the input scaling (K_s, see Fig. 1) was set to 0.08 for both axes. The SRS hexapod motion system supplied the participants with physical roll and pitch motion cues. The motion cues were designed such that the center of rotation is aligned with the subject's vertical body axis and 0.7 m below their design eye position. The time delay of the SRS motion system is 30 ms [25]. To not hear the motion base actuators, participants were asked to wear noise-cancelling headphones.

The only visual cue available for the participants was the display illustrated in Fig. 1. Other visual cues such as the outside visuals were switched OFF. The 15 in cockpit display showing the experiment display had a 1074 by 768 pixels resolution and an image generation delay of around 25 ms. The artificial horizon display was and average of 90 cm away from the participants' eyes and dark brown and blue were used for presenting the ground and sky, respectively. For the single-axis cases, the inactive display axis was locked at 0°. The compensatory display only presents the pitch and roll errors e_θ and e_ϕ, respectively. For any artificial horizon display–where the chosen virtual field of view determines the vertical target line movement due to e_θ, but the target line rotation due to e_ϕ is independent of this field of view–there is a resolution difference in pixels and thereby degree of error illustrated for both axes. For equal e_θ and e_ϕ of 5°, the pixel area swept by the moving target line on our display was 2.3 times larger for pitch than for roll.

3) Participants and Experimental Procedures: Twelve right-handed participants performed the experiment. Half of the invited participants were trained pilots whereas the other half were skilled nonpilots, with extensive experience from earlier experiments. Participants performed a minimum of four to five training runs for every experiment condition to allow their performance to stabilize, eliminating learning effects. Thereafter, five more runs at a constant, fully learned level of performance were collected as the measurement data. Each tracking run lasted 90 s, of which the final 81.92 s were used for data analysis. Participants were instructed to minimize the roll and pitch tracking errors. After each run, the participants were notified of their performance (RMS of the tracking errors), to motivate them to perform consistently.

B. Data Processing

1) Identification Approach: In literature, numerous different methods for the identification of human control dynamics have been proposed and applied, e.g., methods based on autoregressive exogenous identification [26], [27], Kalman filtering [28], [29], and time-domain maximum likelihood estimation [30]. However, these methods, which all fit an assumed LTI model structure to time-domain data, generally result in overdetermined and inconsistent human controller identification results for multiple-input-single-output type systems. This is particularly an issue for human control dynamics characterized by multiple parallel and dynamically similar control responses, as is the case with dual-axis tasks, especially with the added crossfeed dynamics (see Fig. 1). For this reason, in this paper, we rely on an extended frequency-domain Fourier coefficient method [4], [16], which with a total of four independent target and disturbance forcing functions inserted in both axes (see Section III-B) guarantees the successful dissection of the human visual, vestibular and crossfeed responses for each axis. Furthermore, this "black box" identification technique provides a frequency response estimate without requiring any *a priori* assumptions on the actual dynamics of each identified control response.

Fig. 1 illustrates the control diagram of the dual-axis tracking task with motion feedback, with crossfeed between the controlled roll (ϕ) and pitch (θ) axes explicitly accounted for.

In roll, the following expression in the frequency domain can be derived for the total HC control input u_r:

$$U_r(j\omega) = E_r(j\omega)H_{p_{e_r}}(j\omega) + E_p(j\omega)H_{p_{c_p}}(j\omega) + \Phi(j\omega)H_{p_\phi}(j\omega) + N_r(j\omega). \tag{6}$$

The same derivation method can be applied for pitch axis control to obtain a similar equation. For identification of the human operator, (6) would have to be solved for its three unknowns: $H_{p_{e_r}}(j\omega)$, $H_{p_{c_p}}(j\omega)$, and $H_{p_\phi}(j\omega)$. To achieve this, the objective HC identification method developed by [16] has been extended. This method is a frequency-domain identification technique, using Fourier coefficients (FCs), which can be used without any prior knowledge about the dynamics of the system to be identified [31], [32]. The objective identification method by [16] uses *two* independent multisine target and disturbance forcing function signals (e.g., f_{t_r} and f_{d_r} in Fig. 1) to identify *two* human operator responses ($H_{p_{e_r}}$ and H_{p_ϕ} in Fig. 1) in a single-axis task, by interpolating between the frequencies excited by both applied forcing function signals. For the dual-axis task of Fig. 1, a similar method is derived, where for identification of the additional unknown crossfeed response $H_{p_{c_p}}$, additional independent forcing function components *from the other axis* is used. For a successful approach, this requires that all four forcing function signals shown in Fig. 1 be independent, i.e., be composed of sines with different frequencies.

If this requirement is met, following the same procedure as proposed in [16], the following system of three equations may be derived by evaluating (6) at each of the frequencies of f_{t_r}, as well as by interpolating from the frequencies of f_{d_r} and f_{t_p}, as indicated by the superscripted symbols in (7). The interpolation procedure consists of initially removing the forcing function phase from all signals, after which an interpolation of complex

numbers is performed

$$\begin{pmatrix} U_r^{t_r} \\ \tilde{U}_r^{d_r} \\ \tilde{U}_r^{t_p} \end{pmatrix} = \begin{pmatrix} E_r^{t_r} & E_p^{t_r} & \Phi^{t_r} \\ \tilde{E}_r^{d_r} & \tilde{E}_p^{d_r} & \tilde{\Phi}^{d_r} \\ \tilde{E}_r^{t_p} & \tilde{E}_p^{t_p} & \tilde{\Phi}^{t_p} \end{pmatrix} \begin{pmatrix} H_{p_{e_r}} \\ H_{p_{c_p}} \\ H_{p_\phi} \end{pmatrix}. \quad (7)$$

All variables in (7) are a function of the roll target forcing function frequency ($j\omega_{t_r}$), even though this indication is dropped for notation purposes. The system of equations (7) can be solved for $H_{p_{e_r}}(j\omega_{t_r})$, $H_{p_{c_p}}(j\omega_{t_r})$, and $H_{p_\phi}(j\omega_{t_r})$ from inversion of the matrix-vector equation. Furthermore, equivalent frequency response estimates can be obtained at the frequencies of f_{d_r}. This method has been verified successfully using computer simulations.

2) Parameter Estimation: With the obtained FCs of the operator responses, parameter estimation was performed, based on the pilot model structure proposed in Section III-C, and the candidate crossfeed structure to be proposed later in Section V-B. Parameters were estimated by minimizing a cost function $J(\theta)$ that includes the differences between the FCs of the measured data and the frequency response of the pilot model

$$\epsilon(j\omega|\theta) = \frac{|H(j\omega|\theta) - \hat{H}(j\omega)|}{|\hat{H}(j\omega)|} \quad (8)$$

$$J(\theta) = \epsilon(j\omega|\theta)^T W \epsilon(j\omega|\theta). \quad (9)$$

Here, $H(j\omega|\theta)$ is the estimated model as a function of the model parameter vector θ and $\hat{H}(j\omega)$ represent the estimated FCs. The complex error is normalized using the FC estimates to avoid the smaller errors from being ignored. The weighting matrix W was modified such that the outliers can be neglected. These outliers are a consequence of the possible bias introduced during the interpolation of the FCs [7], [16].

3) Model Validation: The variance accounted for (VAF) is a model validation metric in the time domain. Simulated time domain responses u_{mod} of the modeled transfer function are compared to experimental time domain data u_{exp}

$$\text{VAF} = \left(1 - \frac{\sum_{k=1}^{N} |u_{\text{exp}}[k] - u_{\text{mod}}[k]|^2}{\sum_{k=1}^{N} u_{\text{exp}}^2[k]}\right) \times 100\%. \quad (10)$$

It represents the normalized sum of errors in the time domain subtracted from unity, where N is the number of samples. The higher the VAF, the better the model is able to capture the dynamics in the time domain. A VAF of 100% means that the model explains 100% of the measured signal.

C. Dependent Measures

The dependent measures are performance metrics, parameter estimates, crossfeed metrics, and intermittency metrics.

1) Performance Metrics: To compare the level of task performance between single and dual-axis tracking, the variance of the roll and pitch error signals (σ_e^2) is calculated. Calculation of this variance from spectral analysis of the measured signals, allows for separating the individual contributions of the target and disturbance signals, as well those attributable from the target and disturbance signals from the other axis, as all provide power at independent frequencies [15]. Hence, the variance was found by integrating the power spectral density at each forcing function's set of excitation frequencies.

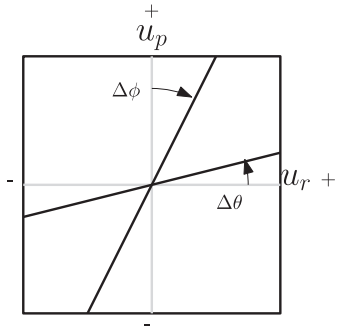

Fig. 2. Two-dimensional control-output plot.

Similarly, the control variance (σ_u^2) is used to quantify differences in control activity between single and dual-axis tasks. To give an indication of the stability of the system, the open-loop target phase margin is calculated. To give an indication of how well, and up to which frequency, the pilot is able to track the target, the target crossover frequency is calculated.

The general open-loop function can be obtained using Fourier transferred experimental signals as given in below equation for roll

$$H_{OL_r}(j\omega_r) = \frac{\Phi(j\omega_r)}{E_r(j\omega_r)}. \quad (11)$$

2) Parameter Estimates: With the parameter estimation method described in Section IV-B2, the parameters of H_{p_e}, H_{p_ϕ}, H_{p_θ}, and H_{p_c} are estimated. These parameters can give additional insight to the underlying principles that define the differences surfaced in the performance metrics.

3) Crossfeed: In the presence of crossfeed, a significant component of the error or control variance can be attributed to the off-axis forcing functions. To analyze the crossfeed dynamics itself, the identification approach elaborated in Section IV-B1 is applied to obtain frequency response estimates of human operators' visual, motion, and crossfeed responses. To quantify the practical significance of the modeled crossfeed, the modeled output contributions of the visual, vestibular, and crossfeed responses, denoted in Fig. 1 by u_e, u_ϕ or u_θ and u_c, respectively, are analyzed and compared. This is done with the parametric models of the three operator response functions. The individual output contribution variances are divided by the total contribution to find the percentage contribution of the separate operator responses. Moreover, the time-domain significance of modeled crossfeed is analyzed by comparing the VAF with and without the modeled crossfeed contribution.

To analyze a possible motoric origin of crossfeed, i.e., how crossfeed may result from hand geometry, two-dimensional (2-D) control output plots are used as given by Fig. 2. Here, the *y*-axis presents the pitch input u_p and the *x*-axis presents the roll input u_r. The angle sign convention is chosen such that positive inputs in the principle axis results in a positive input in the off axis. The relationship between the single axis hand deviation angle ($\Delta\phi$ or $\Delta\theta$) and the corresponding crossfeed gain K_c

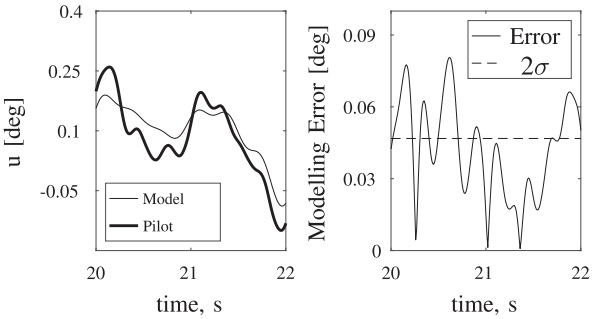

Fig. 3. Illustration of peak time.

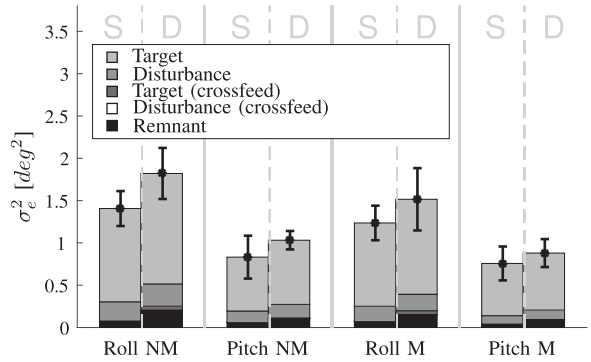

Fig. 4. Error variance decomposition.

obtained from the parameter estimates can give insight about the relationship between motoric and identified crossfeed.

4) Intermittency: Intermittent behavior is not linear and by definition time variant. Therefore, by comparing the single axis VAF to the dual-axis VAF, something can be said about the HC's dual-axis linear time-invariant behavior, or lack thereof.

Intermittency is defined here as the time-varying axis prioritization in multi-axis control. When one axis is ignored, error builds up in that axis, which can result in an aggressive corrective pilot input in that axis, which results in a nonlinear peak. Peak time is defined as the time (equal to the number of instances) in which the modeling error (difference between measured output and simulated model output) is larger than two standard deviations of the baseline single axis modeling error as illustrated in Fig. 3. This calculation however, assumes that the modeling error is normally distributed. To differentiate between pilot noise and intermittency, anything below 2σ is excluded from what is considered peak time. Here, we try to capture the unaccounted-for HC peaks and see how the occurrences of these peaks may change with each condition. This measure is expected to give an indication of intermittency when modeling accuracy is high.

D. Hypotheses

Based on previous investigations, elaborated in the introduction and background sections, we state six hypotheses.

1) Performance degrades in dual-axis tasks compared to the independent single axis tasks, indicated through an increase in error variance, a smaller crossover frequency, and a smaller phase margin [1], [7], [17].
2) Performance degradation in dual axis is smaller with physical motion [10], which can be indicated by a decrease in error variance, an increase in crossover frequency and an increase in phase margin.
3) Asymmetrical human control behavior in each axis can be seen from unequal HC parameters in each axis, as well as from differences in error variance, control variance, crossover frequency, and phase margin between the roll and pitch axis [9], [1].
4) Crossfeed is present in dual-axis manual control [5], [7], which can be found through the presence of off-axis frequencies in principle axis and through the developed FC method.
5) Intermittency is present in dual axis [21], which can be indicated through a consistently lower VAF, and consistently more occurrences of peaks.
6) Intermittency in dual axis is mitigated with motion [10], which can be indicated by a decrease in peak time and an increase in VAF.

V. Results

This section contains four main parts: performance metrics, crossfeed describing function, parameter estimation, crossfeed, and intermittency. The *performance* metrics bring forth the higher level distinction between single and dual-axis manual control. The *crossfeed describing function* presents the crossfeed FCs along with a candidate structure that fits the dynamics of crossfeed. After which the *parameter estimation* and *crossfeed* sections bring about the underlying mechanisms that cause differences between single and dual axis to occur. Finally, the *intermittency* section analyzes the linearity of the system and the intensity of intermittent peaks. Three-way analyses of variance (ANOVAs) have been performed with axis type (pitch or roll), axis dimension (single or dual), and motion as factors. Significant ANOVA results are mentioned in text. Although two subject groups were tested: pilot and nonpilot, none of the between-subjects effects were significant, therefore only the results of a full repeated-measures (within subjects) ANOVA are presented. The ANOVA is reported through an F-statistic, with its associated degrees of freedom between brackets, and the corresponding p-value.

A. Performance Metrics

To evaluate performance, there are four metrics of interest; error variance, control variance, crossover frequency, and phase margin. These are presented in Figs. 4, 5, 6, and 7, respectively.

Figs. 4 and 5 show the average roll and pitch axis error and control signal variances. These variances are composed of contributions from the signals of the principle axis, off-axis and human operator remnant contributions. Variances are shown for pitch and roll control separately, also indicating the presence of motion with an ("M") and no motion case with ("NM"). Furthermore, the left bar of each set of two corresponds to the

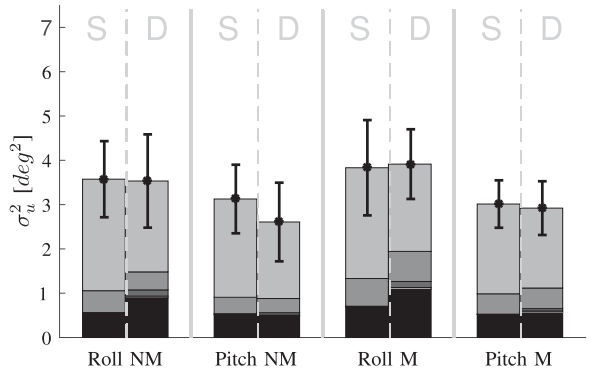

Fig. 5. Control variance decomposition.

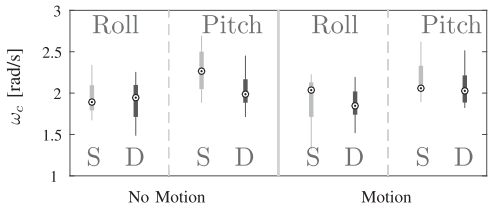

Fig. 6. Boxplot representation of single and dual-axis crossover frequency.

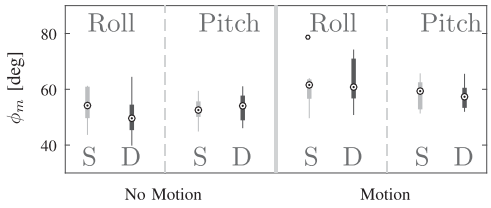

Fig. 7. Boxplot representation of single and dual-axis phase margin.

single-axis task ("S"), while the right data are from the dual-axis task ("D").

From Fig. 4, the performance is significantly worse for dual axis ($F(1,11) = 6.8$, $p \leq 0.05$). This can be attributed to three components; an increase in remnant ($F(1,11) = 5.031, p \leq 0.05$), as well as the added off-axis target and disturbance (crossfeed) contributions $\sigma_{f_{to}}$ ($F(1,11) = 26.5, p \leq 0.01$), and $\sigma_{f_{do}}$ ($F(1,11) = 6.2, p \leq 0.05$), respectively.

Performance in roll is worse than that in pitch ($F(1,11) = 71.3$, $p \leq 0.01$), shown through significantly larger target ($F(1,11) = 62.8$, $p \leq 0.01$), disturbance ($F(1,11) = 93.7$, $p \leq 0.01$), of target ($F(1,11) = 11.9$, $p \leq 0.01$), and remnant contributions ($F(1,11) = 9, p \leq 0.05$). A possible cause for this discrepancy is the decreased perceivability of roll errors due to the lower pixel resolution used. Moreover, there is significantly larger remnant ($F(1,11) = 15.1$, $p \leq 0.01$) and off-axis target ($F(1,11) = 9.9$, $p \leq 0.01$) contribution for dual-axis roll than for pitch resulting in a significant overall performance interaction ($F(1,11) = 6.6$, $p \leq 0.05$).

The presence of simulator motion reduces both the target and disturbance contributions: ($F(1,11) = 16, p \leq 0.01$) ($F(1,11) = 27.1$, $p \leq 0.01$), for both axes types and dimensions. Motion adds more value to the roll axis than to the pitch axis. This interaction ($F(1,11) = 7.4$, $p \leq 0.05$) stems mainly from the target contribution, as this contribution decreases more when motion is added to the roll axis.

Although the total control variance (see Fig. 5), is not significantly affected by the number of controlled axes or by motion, some of its contributions are. At approximately the same level of total control variance for dual axis, the target contribution decreases ($F(1,11) = 7.7, p \leq 0.05$), at increased levels of other contributors. For the pitch axis there is significantly larger off-axis target ($F(1,11) = 43.2, p \leq 0.01$) and disturbance ($F(1,11) = 6.4$, $p \leq 0.05$), whereas for roll, in addition to the off-axis contributions, there is a significant increase in remnant noise, reflected in a significant interaction ($F(1,11) = 15.6, p \leq 0.01$). This shows that the dual-axis roll axis inputs are noisier than that of dual-axis pitch.

The roll axis has a significantly higher control variance ($F(1,11) = 15.3$, $p \leq 0.01$) than that of the pitch axis, which stems from significantly larger target ($F(1,11) = 9.8, p \leq 0.05$), disturbance ($F(1,11) = 24.6$, $p \leq 0.01$), and remnant ($F(1,11) = 9.9, p \leq 0.05$) contributions. The reason for such a difference could be due to hand force asymmetry and hand geometry, it could be easier to make larger deflections in the roll axis of the manipulator stick used. The addition of motion increases the subjects' reaction to the disturbance signal ($F(1,11) = 30$, $p \leq 0.01$), moreover the disturbance contribution is slightly higher for dual-axis motion than for single axis ($F(1,11) = 5.1$, $p \leq 0.05$). The enhancement of disturbance contribution with motion is in line with previous research [33].

Following the open-loop calculation outlined in Section IV, Figs. 6 and 7 show the crossover frequency and phase margin of the open-loop system. These data are presented using boxplots, where the central mark indicates the median, the bottom and top edges the 25th and 75th percentiles, and the whiskers show the complete data range excluding outliers. Crossover frequency reduces significantly in the dual-axis conditions ($F(1,11) = 5$, $p \leq 0.05$), as hypothesized. It can be seen that ω_c is higher in the pitch axis than in the roll axis ($F(1,11) = 21.3$, $p \leq 0.01$). This inclination towards performing better in pitch indicates axis asymmetry.

The phase margin is not affected by the axis dimension, nor is it consistently different for pitch or roll. It is only significantly affected by motion ($F(1,11) = 30.9, p \leq 0.01$). This is in line with a previous investigation by [33], which found that for target tracking tasks, the phase margin increases with motion, implying increased stability with motion. Although there is a steady increase in phase margin for all conditions, the increase of dual-axis roll from 47° to 63° on average, is significantly larger, which is reflected in the significant interaction between axis dimension and motion ($F(1,11) = 15.1, p \leq 0.01$).

B. *Crossfeed Describing Function*

Using the identification method described in Section IV-B1, the frequency responses of the operator visual, vestibular, and crossfeed responses were estimated. Fig. 8 shows the roll-axis human operator responses identified for Subject 2. The red stars present the identified frequency response, with the

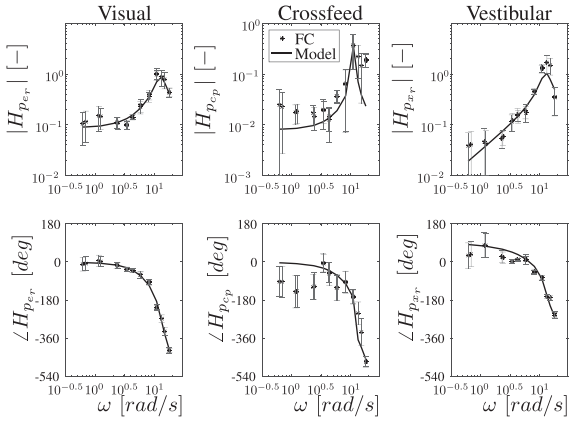

Fig. 8. Roll-axis human operator frequency response estimates (Subject 2, dual-axis task) with visual response (left), crossfeed response (center), and motion response (right). The model responses are based on a model structure that is described in Section V-B, with model parameters estimated in Section V-C.

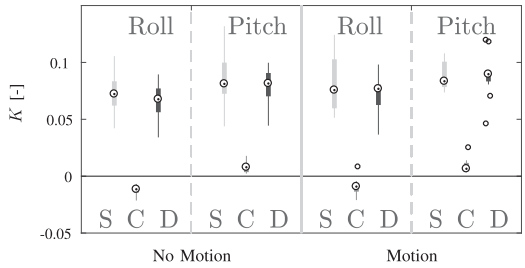

Fig. 9. Single, crossfeed, and dual-axis values for operator gain.

errorbars showing the 95% confidence intervals over the five measurement runs.

Fig. 8 shows consistent estimation of the dynamics of all three responses. Furthermore, in partial confirmation of earlier results [5], [7], the dynamics of the crossfeed response appear to be very similar to those of the visual response, however, with a lower gain and a 180° phase shift. This makes sense because the input to the crossfeed response is visual cue. Based on these observations, a candidate model structure for the crossfeed response, to complement well-known models for the visual and vestibular responses [4], [23], would be identical to the visual response model, as given by

$$H_{p_{c_p}} = \frac{K_{cp}(1 + T_{L_{c_p}} s)\omega^2_{\text{nm}_{c_p}}}{\omega^2_{\text{nm}_{c_p}} + 2\zeta_{\text{nm}_{c_p}}\omega_{\text{nm}_{c_p}} s + s^2} e^{-s\tau_{c_p}}. \qquad (12)$$

C. Parameter Estimates

With the parameter estimation method described in Section IV-B2, the parameters of H_{p_e}, H_{p_ϕ}, or H_{p_θ} and H_{p_c} were estimated. In total, 24 parameters could be estimated for a dual-axis run with motion. These can give insight to the human adaptation that causes the differences surfaced in the performance measures. It will also clarify whether a completely independent crossfeed transfer function is necessary.

Two parameter types have shown significant effects and are of interest namely; the gains (K_v and K_c) and time delays (τ_v and τ_c) shown in Figs. 9 and 10, respectively. Whereas the parameters without significant effects are the following along with their range of values: lead time constants T_l (0.4s ± 0.2s), neuromuscular damping η_{nm} (0.3 ± 0.15), neuromuscular frequency ω_{nm} (12 rad/s ± 3 rad/s), motion gains K_m (0.012 ± 0.01), and motion time delays τ_m (0.22 s ± 0.08 s).

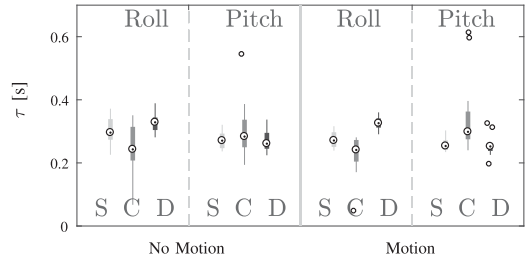

Fig. 10. Single, crossfeed and dual-axis values for visual time-delay.

1) Gains: The gains are illustrated in Fig. 9, presenting the single and dual-axis visual gains K_v, and crossfeed gain K_c. The axis type has a significant effect on the visual gains, with the pitch axis having a larger gain than roll ($F(1,11) = 22.1$, $p \leq 0.01$). Here, we can see that due to the higher gain for pitch by default (also for single axis), the pitch errors are corrected more strongly than the roll errors.

The crossfeed gains K_c, Fig. 9 are significantly affected by axis type ($F(1,11) = 132.4$, $p \leq 0.01$), not only in terms of magnitude but also in terms of sign (being negative or positive). The absolute roll crossfeed gain is also higher than the absolute pitch crossfeed gain. This means that there is a stronger component of pitch in the roll axis than vice versa, which corresponds with Figs. 4 and 5. In line with the negative roll axis cross-feed gain, the phase of the crossfeed frequency response in Fig. 8 has indeed a $-180°$ phase shift. The reasons for the gain's negative sign in relation to crossfeed will be further elaborated in Section V-D.

2) Time Delays: The time delay plot shown in Fig. 10 illustrates the single and dual axis' τ_v and crossfeed delay τ_c. Parameter τ_v is significantly different for single and dual-axis tasks ($F(1,11) = 9.6$, $p \leq 0.05$), as well as for pitch and roll tracking ($F(1,11) = 98.9$, $p \leq 0.01$). This is illustrated by the roll axis having a clearly higher dual-axis delay, whereas the pitch axis delay is relatively unaltered. A higher delay for dual axis is an expected result, as it takes longer to perceive and process two degrees of freedom simultaneously [7], [17].

The crossfeed time delay τ_c is comparable to the off-axis visual time delay. This means that τ_{c_r} is comparable to τ_{v_p}. This suggests linking the crossfeed time delay parameter with the visual time delay of the other axis, as crossfeed takes as input the visually perceived error of the off axis. The formalization and further validation of this observation is left for future studies.

D. Crossfeed and its Contribution

The presence of off-axis forcing function contributions in Figs. 4 and 5 is clear evidence of the presence of crossfeed between the roll and pitch tasks.

Crossfeed can have motoric and perceptual origins. Evidence that the crossfeed we are considering has a primarily *motoric*

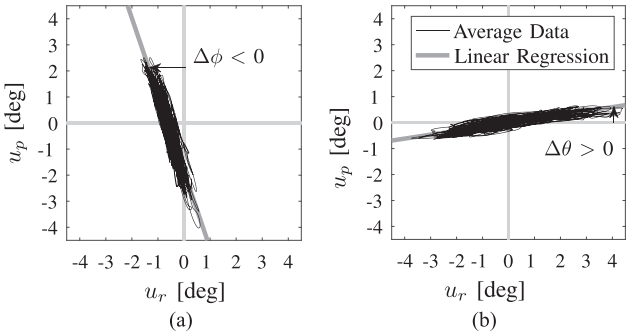

Fig. 11. Two-dimensional control input plots (Subject 1). (a) Single-axis pitch. (b) Single-axis roll.

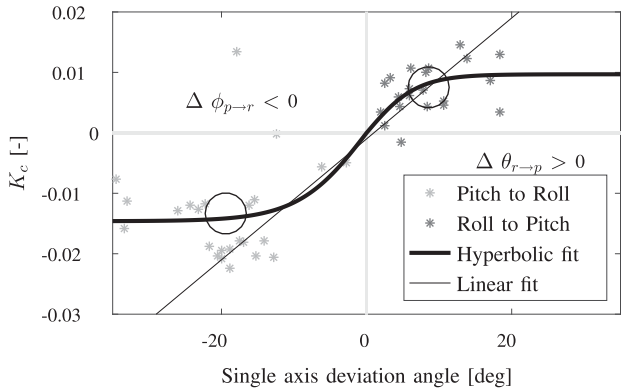

Fig. 12. Crossfeed motoric single axis crossfeed slope versus its dual-axis gain.

component can be seen in Fig. 11, which shows that Subject 1's single-axis control inputs were not perfectly aligned with the sidestick's natural axis. Both a slope and bias is present, with the slope having a relationship with crossfeed gain as given in Fig. 12 and the HC's bias being arbitrary.

The single axis pitch control input in Fig. 11(a) shows a (negative) slope, implying that for every pitch input, a small coupled negative input in roll was given. From Fig. 12, it is clear that this is the case for most subjects. Fig. 11(b) shows that this participant showed a similar, yet reduced, crossfeed from roll to pitch. These observations are in line with the differences in the magnitude and sign of K_c shown in Fig. 9. The orientation of the fitted linear regression for the pitch task confirms that for a positive u_p, a negative u_r was given. This is also consistent with the -180° phase shift observed for the crossfeed response in Fig. 8 and the negative K_c values obtained for the roll axis. These results reveal that participants are unable to fully decouple the pitch and roll-axis tasks at the manipulator level, likely due to hand geometry.

Although one may be inclined to postulate such a relation, there is no linear one-to-one correspondence between the motoric single axis hand deviation angle as given in Fig. 11 and the crossfeed gain. In Fig. 12, the pitch-to-roll gains are negative and correspond to a negative single axis pitch to roll hand deviation angle, whereas the positive roll to pitch crossfeed deviation

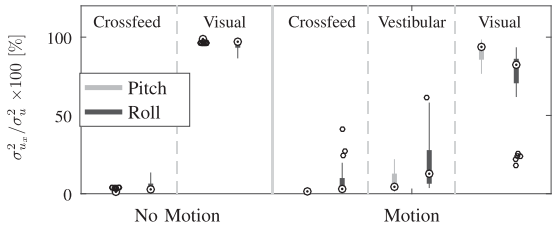

Fig. 13. Fractions of control input variance explained by modeled visual, vestibular, and crossfeed responses.

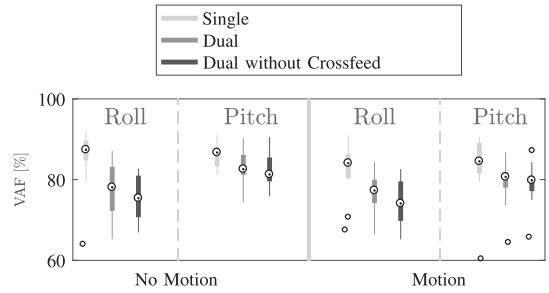

Fig. 14. Variance accounted for of the single and dual-axis modeling fits, additionally: the dual axis with modeled crossfeed.

angle corresponds to a positive pitch crossfeed gain. Additionally, we included a circle in this figure to indicate the average gain and deviation angles for both roll and pitch crossfeed. It is interesting that the average motoric off-axis stick deflection is 8.5° for roll and 17.2° for pitch, suggesting that our hand naturally tends to give more inputs from pitch to roll. The linear line included in Fig. 12 has a correlation coefficient of 0.81, whereas the nonlinear hyperbolic tangent function (thick line) has a correlation coefficient of 0.89. Although it is difficult to make conclusions about the nature of the relationship, the pattern suggests that up to a certain amount of motoric crossfeed, due to a motoric deflection angle, the crossfeed gain K_c will not further increase, as if there is a saturation limit. Possibly, past this saturation limit, the additional cross feed is fully taken as noise. Clearly, more work is needed on this topic.

From the full human operator model fits, the percentage of the total modeled control signal's variance explained by the different human operator responses was calculated for each participant and is shown in Fig. 13. While the modeled contribution of the crossfeed response $\sigma^2_{u_c}$ to the total operator input σ^2_u is seen to be relatively minor compared to the visual $\sigma^2_{u_v}$ and vestibular $\sigma^2_{u_m}$ contributions, it still can be quite significant with values up to 20%–30% for the roll axis with motion. The presence of simulator motion decreases the relative visual contribution $\sigma^2_{u_v}$ by increasing both the vestibular and crossfeed contributions.

The added value of the modeled crossfeed is evident from the statistically significant variance accounted for (VAF) contribution ($F(1,11) = 10.8$, $p \leq 0.01$) presented in Fig. 14. Although the contribution may be small (1%–5% increase), it is consistent, proving a modeling improvement.

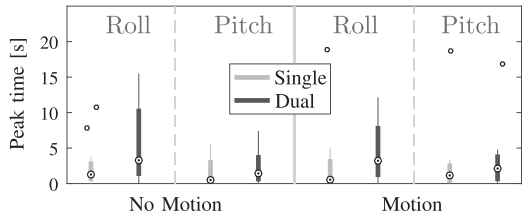

Fig. 15. Peak time.

E. Intermittency

The VAF and peak time can both reveal a lack of linear time-invariant behavior, a possible intermittency. It can be seen from Fig. 14 that the VAF is significantly lower for dual-axis runs. Although the VAF shows consistently lower values for both roll and pitch dual-axis tasks, the peak time in Fig. 15 only seems to increase for roll dual axis. Using Friedman's test it is found that there is a statistically significant difference between the conditions for peak time ($\chi^2(7) = 16.69$, $p = 0.02$), and using Wilcoxon's signed rank test it is found that the peak time for dual-axis roll without motion is significantly larger than single-axis roll with motion ($Z = -2.22$, $p = 0.026$). An indication of less linear behavior in the dual-axis roll is also visible in the VAF plot, as dual-axis roll shows the lowest VAF of all conditions.

VI. Discussion

A human-in-the-loop experiment was performed in a moving-base simulator to investigate four phenomena in dual-axis manual control: performance degradation, axis asymmetry, crossfeed, and intermittency. The effects of simulator motion on these four phenomena were also studied. Data were collected from twelve participants performing a compensatory roll and pitch tracking task with fully independent target and disturbance forcing functions in each controlled axis. In addition to the dual-axis condition, reference measurements of the corresponding single-axis pitch and roll tracking behavior were collected for direct comparison.

It has been found that dual-axis control behavior induces more error and thereby *performance degradation*, in line with previous studies [7], [17]. Suggesting that whilst the HC distributes their attention over multiple channels, the performance in a single channel decreases. Interestingly, the control variance remains the same. The HC reacts to off-axis target and noise, reducing the operator's response to the principal axis' target and disturbance, evident from the distributed control variance. This finding is in line with [6], which suggests the modeled human is adapted by only increasing its remnant noise with the number of axis used. Performance degradation is also reflected in the decreased crossover frequency. Whereas some studies suggest a degradation ratio in relation to the corresponding single axis ω_c such as $1/\sqrt{2}$ [10], such a consistent ratio has not been found here.

Although the control variance in the roll axis is significantly higher than in pitch, performance is always worse, indicating *axis asymmetry*. The consistently higher crossover frequency and decreased error variance in pitch for both the dual and single-axis cases compared to roll, shows that there is a preference. Earlier experiments [1], [9] state that human operators tend to show markedly worse performance in roll in dual-axis tasks, even for identical task settings. Hence, this was evident from in the visual time delay of single axis roll being larger than for pitch, moreover, with dual axis the roll time delay decreases even more, with pitch time delay staying constant. A possible cause is the artificial horizon display used: pitch errors having a resolution that has a factor of 2.3 pixels more than roll, per degree. When predicting human performance for dual-axis tasks, awareness of such display design choices is a factor that is important to account for.

Motion was found to significantly improve performance by decreasing error variance and improve stability, in line with [23] and [33]. Contrary to previous studies [10], this investigation has not found a significant effect of motion on crossover frequency or time delay. This unexpected result stems from the second-order controlled element considered. A break frequency of 3 rad/s ensures that the controlled dynamics approximates a single integrator in the main operating bandwidth, meaning that the full benefits of motion could not be fully realized. Hence, it is possible that the lack of significance of motion on intermittency and crossfeed could be due to our choice of dynamics.

Crossfeed has been successfully detected, identified and modeled in this paper. The explicit identification was made possible through an extension of the FC method in [16]. Due to the crossfeed block allowing for a flow of excitation frequencies between axes', this opens up opportunities for identifying a maximum of four operator response functions per axis. In this paper, however, only three blocks where identified, where a choice was made on the used excitation frequency set based on their signal power.

The HC modeling results including crossfeed show that the crossfeed contributes up to 20% of the total human control response, and that the addition of crossfeed improves the accuracy of the time-domain modeling by up to 5%, thereby suggesting crossfeed as a key attribute of human multi-axis control. The crossfeed candidate structure used in this paper is similar to that of the visual response structure. If the crossfeed response is purely motoric, one would expect identical parameter settings as found for the off-axis visual response. The results of the parameter estimates suggest that although the crossfeed gain K_c has a different range of values for the principle and off axes, the time delay parameter τ_c could be approximated as its off-axis parameter. Nevertheless, to obtain a firm grasp on the needed parameters for crossfeed modeling, a parameter sensitivity analysis would be beneficial for the future. As not all crossfeed parameters can be simplified, the crossfeed response can be seen as quasi independent from the off-axes responses, meaning that the crossfeed response is not fully motoric as it can also have a perceptual contribution.

As a consequence of hand geometry, the participant suffered from motoric crossfeed as evident from the 2-D input plots. However, there also exists crossfeed axis asymmetry, which is a consequence of both the nature of the visual display and the hand geometry. The roll crossfeed gain (a contribution from the pitch axis) is larger than the respective pitch crossfeed contribution from the roll axis. This difference in contribution can also be

seen from the distributed variance plots and the modeled output crossfeed contribution $\sigma^2_{u_c}$. Although the control input in the roll axis is larger, which may be due to hand force asymmetry [34], the crossfeed contribution to the roll axis is found to be larger. The likely reason for a larger roll crossfeed contribution is hand geometry; the average motoric crossfeed from pitch to roll is larger, suggesting that through our hand-arm posture, there are more inputs from pitch to roll.

Intermittency is a type of time-varying axis prioritization, which, in combination with crossfeed can be difficult to detect. Previous studies indicate that the axis with the largest errors is often prioritized [9], [1]. This type of time variant, nonlinear behavior is traditionally modeled as additional pilot remnant. This study has found larger pilot output remnant for dual-axis roll than that for single-axis roll, which can be attributable to intermittency, as the averaged peak times for roll dual axis are significantly larger than that for single axis. Furthermore, since the modeling accuracy in the time domain is at an acceptably high level, it can be said that the peak time analysis gives a clear indication of intermittency. The consistently degraded VAF for dual-axis tracking indicates that dual-axis manual control is less linear-time-invariant. The cause for such intermittent behavior, especially for the roll axis, could be attributable to the display signals' perceivability, however this needs more investigation. Therefore, it is recommended to investigate the cause of intermittency to identify its nature and possibly nonlinear task interference effects using more sophisticated nonlinear techniques.

VII. Conclusion

In this paper, the existence of performance degradation, axis asymmetry, crossfeed, and intermittency in dual-axis tasks, and the effect of motion on these occurrences were investigated. It has been found that performance degradation occurs in dual-axis tasks, with an increase in error variance and a decrease in crossover frequency, however this degradation is larger for roll than it is for pitch which surfaces evidence for axis asymmetry. Motion improves stability and error variance for both single and dual-axis cases. Crossfeed is successfully detected using spectral analysis and was identified using a novel extended FC method. With a maximum contribution of 20%, and an improvement of modeled dual-axis behavior by up to 5%, the crossfeed's contribution is significant, and is, therefore, an important phenomenon to consider for dual-axis manual control modeling. Dual-axis tracking is less linear and less time invariant than single-axis tracking. This difference appears to arise from intermittency.

References

[1] G. Bekey, H. Meissinger, and R. Rose, "Mathematical models of human opertors in simple two-axis manual control systems," *IEEE Trans. Human Factors Electron.*, vol. HFE-6, no. 1, pp. 42–52, Sep. 1965.

[2] D. T. McRuer, D. Graham, E. S. Krendel, and W. J. Reisener, "Human Pilot dynamics in compensatory systems, theory models and experiments with controlled element and forcing function variations," Air Force Flight Dynamics Laboratory, Wright-Patterson Air Force Base, Wright-Patterson Air Force Base, OH, USA, Tech. Rep. AFFDL-TR-65-15, 1965.

[3] D. T. McRuer and H. R. Jex, "A review of quasi-linear pilot models," *IEEE Trans. Human Factors Electron.*, vol. HFE-8, no. 3, pp. 231–249, Sep. 1967.

[4] R. L. Stapleford, D. T. McRuer, and R. E. Magdaleno, "Pilot describing function measurements in a multiloop task," *IEEE Trans. Human Factors Electron.*, vol. 8, no. 2, pp. 113–125, Jun. 1967.

[5] E. Todosiev, "Human performance in a cross-coupled tracking system," *IEEE Trans. Human Factors Electron.*, vol. HFE-8, no. 3, pp. 210–217, Sep. 1967.

[6] W. H. Levison, J. I. Elkind, and J. L. Ward, "Studies of multivariable manual control systems: A model for task interference," NASA, Washington, D.C, USA, Tech. Rep. NASA CR 1746, 1971.

[7] A. Van Lunteren, "Identification of human operator describing function models with one or two inputs in closed loop systems," Ph.D. dissertation, Mechanical Engineering, TU Delft, Delft, The Netherlands, 1979.

[8] A. Karniel and G. F. Inbar, "Human motor control: Learning to control a time-varying, nonlinear, many-to-one system," *IEEE Trans. Syst., Man, Cybern., C, Appl. Rev.*, vol. 30, no. 1, pp. 1–11, Feb. 2000.

[9] D. G. Mitchell, B. L. Aponso, and R. H. Hoh, "Minimum flying qualities, volume I: Piloted simulation evaluation of in multiple axis flying qualities," Flight Dynamics Laboratory, Wright-Patterson AFB, Wright-Patterson Air Force Base, OH, USA, Tech. Rep. WRDC-TR-89-3125, 1990.

[10] H. P. Bergeron, J. J. Adams, and G. J. Hurt, "The effects of motion cues and motion scaling on one and two-axis compensatory control tasks," NASA Langley Research Center, Hampton, VA, USA, Tech. Rep. TN D-6110, 1971.

[11] R. A. Hess, "Analytical assessment of performance, handling qualities, and added dynamics in rotorcraft Flight Control," *IEEE Trans. Syst., Man, Cybern., A, Syst. Humans*, vol. 39, no. 1, pp. 262–271, Jan. 2009.

[12] S. Barendswaard, D. M. Pool, and M. Mulder, "Human crossfeed in dual-axis manual control with motion feedback," in *Proc. 13th IFAC Symp. Human-Mach. Syst.*, Kyoto, Japan, 2016, vol. 49, no. 19, pp. 189–194.

[13] R. Prouty, "Crosscouplings: Its effects on helicopter flight," *Flight Safety Found., Helicopter Saf.*, vol. 15, no. 3, pp. 1–4, 1989.

[14] M. Mulder *et al.*, "Manual control cybernetics: State-of-the-art and current trends," *IEEE Trans. Human-Mach. Syst.*, vol. 48, no. 5, pp. 468–485, Oct. 2018.

[15] H. R. Jex, R. E. Magdaleno, and A. M. Junker, "Roll tracking effects of G-vector tilt and various types of motion washout," in *Proc. 14th Ann. Conf. Manual Control*, 1978, pp. 463–502.

[16] M. M. Van Paassen and M. Mulder, "Identification of human operator control behaviour in multiple-Loop tracking tasks," in *Proc. 7th IFAC/IFIP/IFORS/IEA Symp. Anal., Des. Eval. Man-Mach. Syst.*, Kyoto Japan, 1998, vol. 31, no. 26, pp. 455–460.

[17] W. H. Levison and J. I. Elkind, "Two-dimensional manual control systems with separate displays," *IEEE Trans. Human Factors Electron.*, vol. HFE-8, no. 3, pp. 202–209, Sep. 1967.

[18] J. J. Adams, H. P. Bergeron, and G. J. Hurt, "Human transfer functions in multi-axis and multi-loop control system," NASA Langley Research Center, Hampton, VA, USA, Tech. Rep. TN D-3305, 1966.

[19] S. Baron and W. Levison, "An optimal control methodology for analyzing the effects of display parameters on performance and workload in manual flight control," *IEEE Trans. Syst., Man, Cybern.*, vol. SMC-5, no. 4, pp. 423–430, Jul. 1975.

[20] D. Kleinman, "Solving the optimal attention allocation problem in manual control," *IEEE Trans. Autom. Control*, vol. AC-21, no. 6, pp. 813–821, Dec. 1976.

[21] J. Smisek, E. Sunil, M. van Paassen, D. Abbink, and M. Mulder, "Neuromuscular-system-based tuning of a haptic shared control interface for UAV teleoperation," *IEEE Trans. Human-Mach. Syst.*, vol. 47, no. 4, pp. 449–461, Aug. 2017.

[22] M. Olivari, F. Nieuwenhuizen, J. Venrooij, H. Bulthoff, and L. Pollini, "Methods for multiloop identification of visual and neuromuscular pilot responses," *IEEE Trans. Cybern.*, vol. 45, no. 12, pp. 2780–2791, Sep. 2015.

[23] P. M. T. Zaal, D. M. Pool, J. de Bruin, M. Mulder, and M. M. van Paassen, "Use of pitch and heave motion cues in a pitch control task," *J. Guid., Control, Dyn.*, vol. 32, no. 2, pp. 366–377, 2009.

[24] H. J. Damveld, G. C. Beerens, M. M. Van Paassen, and M. Mulder, "Design of forcing functions for the identification of human control behavior," *J. Guid., Control, Dyn.*, vol. 33, no. 4, pp. 1064–1081, 2010.

[25] W. R. Berkouwer, O. Stroosma, M. M. van Paassen, M. Mulder, and J. A. Mulder, "Measuring the performance of the SIMONA research simulator's motion system," in *Proc. AIAA Model. Simul. Technologies Conf. Exhib.*, San Francisco, CA, USA, Aug. 2005, pp. 2005–6504.

[26] T. Pilutti and A. G. Ulsoy, "Identification of driver state for lane-keeping tasks," *IEEE Trans. Syst., Man, Cybern.*, vol. 29, no. 5, pp. 486–502, Sep. 1999.
[27] F. M. Drop, D. M. Pool, M. M. van Paassen, M. Mulder, and H. H. Bülthoff, "Objective model selection for identifying the human feedforward response in manual control," *IEEE Trans. Cybern.*, vol. 48, no. 1, pp. 2–15, Jan. 2018.
[28] E. R. Boer and R. V. Kenyon, "Estimation of time-varying delay time in nonstationary linear systems: An approach to monitor human operator adaptation in manual tracking tasks," *IEEE Trans. Syst., Man, Cybern.–A, Syst. Humans*, vol. 28, no. 1, pp. 89–99, Jan. 1998.
[29] A. Popovici, P. M. T. Zaal, and D. M. Pool, "Dual extended kalman filter for the identification of time-varying human manual control behavior," in *Proc. AIAA Model. Simul. Technol. Conf.*, Denver, CO, 2017, Paper AIAA-2017–3666.
[30] P. Zaal, D. Pool, P. Chu, Q, M. M. van Paassen, M. Mulder, and J. Mulder, "Modeling human multimodal perception and control using genetic likelihood estimation," *J. Guid., Control, Dyn.*, vol. 32, no. 4, pp. 1089–1099, 2009.
[31] F. Drop, D. Pool, H. Damveld, M. van Paassen, and M. Mulder, "Identification of the feedforward component in manual control with predictable target signals," *IEEE Trans. Cybern.*, vol. 43, no. 6, pp. 1936–1949, Dec. 2013.
[32] K. van der El, D. Pool, H. Damveld, M. van Paassen, and M. Mulder, "An empirical human controller model for preview tracking tasks," *IEEE Trans. Cybern*, vol. 46, no. 11, pp. 2609–2621, Nov. 2016.
[33] D. M. Pool, M. Mulder, M. M. van Paassen, and J. C. van der Vaart, "Effects of peripheral visual and physical motion cues in roll-axis tracking tasks," *J. Guid., Control, Dyn.*, vol. 31, no. 6, pp. 1608–1622, 2008.
[34] R. Hess, "Analyzing manipulator and feel system effects in aircraft flight control," *IEEE Trans. Syst., Man, Cybern.*, vol. 20, no. 4, pp. 923–931, Jul./Aug. 1990.

Sarah Barendswaard received the M.Sc. (*cum laude*) degree in aerospace engineering from TU Delft, The Netherlands, in 2016, for her research on manual control behavior in dual-axis tracking tasks. She is currently working toward the Ph.D. degree with the section Cognitive Robotics, Mechanical Engineering, TU Delft, focuseing on measuring and modeling human driving behavior to adapt haptic driver assistance systems in real time.

Her current research interests include mathematical modeling, system identification, and haptics.

Daan Marinus Pool (M'09) received the M.Sc. and Ph.D. (*cum laude*) degrees in aerospace engineering from TU Delft, The Netherlands, in 2007 and 2012, respectively.

He is currently an Assistant Professor with the section Control and Simulation, Aerospace Engineering, TU Delft. His research interests include cybernetics, manual vehicle control, simulator-based training, and mathematical modeling, identification, and optimization techniques.

Marinus (René) M. van Paassen (M'08–SM'15) received the M.Sc. and Ph.D. degrees in aerospace engineering from TU Delft, The Netherlands, in 1988 and 1994, respectively, for his studies on the role of the neuromuscular system of the pilot's arm in manual control.

He is currently an Associate Professor with the section Control and Simulation, Aerospace Engineering, TU Delft, working on human-machine interaction and aircraft simulation. His work on human-machine interaction ranges from studies of perceptual processes and manual control to complex cognitive systems. In the latter field, he applies cognitive systems engineering analysis (abstraction hierarchy and multilevel flow modeling) and ecological interface design to the work domain of vehicle control.

Dr. van Paassen is an Associate Editor of the IEEE TRANSACTIONS ON HUMAN-MACHINE SYSTEMS.

Max Mulder (M'14) received the M.Sc. and Ph.D. (*cum laude*) degrees in aerospace engineering from TU Delft, The Netherlands, in 1992 and 1999, respectively, for his work on the cybernetics of tunnel-in-the-sky displays.

He is currently a Full Professor and the Head of the section Control and Simulation, Aerospace Engineering, TU Delft. His research interests include cybernetics and its use in modeling human perception and performance, and cognitive systems engineering and its application in the design of "ecological" interfaces.